Stationary Negative Ion Beam Injector for a Tandem Accelerator[1]

A. A. Gmyrya[a],*, Yu. I. Belchenko[a], A. L. Sanin[a], S. S. Savinov[a], S. Yu. Taskaev[a], and I. M. Shchudlo[a]

[a]*Budker Institute of Nuclear Physics, Siberian Branch, Russian Academy of Sciences, Novosibirsk, 630090 Russia*

*e-mail: anatoliigmyrya@gmail.com

Abstract—The results of the work of a new injector for a stationary beam of negative hydrogen ions, put into operation in 2022 at a tandem accelerator with vacuum insulation at the Institute of Nuclear Physics, Siberian Branch, Russian Academy of Sciences, are presented. The injector uses a surface plasma source (SPS) with a Penning discharge with massive heat-resistant electrodes and an internal permanent magnet magnetic system. Source power systems provide feedback and automated control of source operation according to a scenario selected by the operator. The source makes it possible to obtain stationary beams of negative hydrogen ions with a current of up to 15 mA and an energy of up to 32 keV. An additional magnetic lens is installed in the low-energy tract of the injector; to reduce stripping of the negative ion beam, pumping of the low-energy tract is enhanced.

1. INTRODUCTION

The Budker Institute of Nuclear Physics, Siberian Branch, Russian Academy of Sciences, has developed and is actively using an accelerator neutron source for boron neutron capture therapy (BNCT) with acceleration of the primary beam of negative ions in tandem with vacuum insulation (VITA) [1]. From 2006 to 2021, an experimental stationary source of negative ions of the surface-plasma type, developed at the Budker Institute of Nuclear Physics, successfully operated on the tandem, which provided injection of a beam of negative ions with a current of up to 10 mA into the tandem [2]. In 2022, the tandem negative ion injection scheme was improved. The new injection scheme was equipped with a more powerful surface plasma source (SPS) with a Penning discharge, which allows for obtaining stationary beams of negative hydrogen ions with a current of up to 15 mA and an energy of up to 32 keV [3]. Ion source power supply systems provide feedback and automated control of source operation. An additional magnetic lens is installed in the low-energy path of the injector to improve the passage of the beam through the path. Pumping of the low-energy path with additional pumps to reduce stripping of the negative ion beam has been improved.

2. INJECTOR DESIGN

The general diagram of the new injector is shown in Fig. 1. The main components of the injector are a source of negative ions, attached via an adjustment unit to a differentially pumped chamber, inside which the first lens on permanent magnets is installed.

The differentially pumped chamber with lens is attached to the low-energy path of the tandem, which contains an external adjustable solenoid lens that further focuses the ion beam. A pair of correctors is installed behind the solenoidal lens to regulate the angle of entry of the beam into the tandem (not shown in Fig. 1). For differential pumping of hydrogen leaving the source, a stainless-steel cone with an inlet aperture of 40 mm in diameter is used, which separates two pumping stages, each of which is equipped with a turbomolecular pump with a hydrogen pumping rate of 2200 L/s. With a steady flow of hydrogen at a rate of approximately 0.1 L Torr/s, pumps maintain a vacuum of approximately 2.2×10^{-5} Torr in the first stage adjacent to the source and approximately 10^{-5} Torr in the LEBT transport chamber. An additional turbomolecular pump with a pumping speed of 2000 L/s is installed at the tandem input. The beam diagnostics are performed using an oscillating wire scanner and an emittance meter from D-Pace installed in the diagnostic chamber. The red lines in Fig. 1 show the trajectories of the 32 keV beam ions as they move from
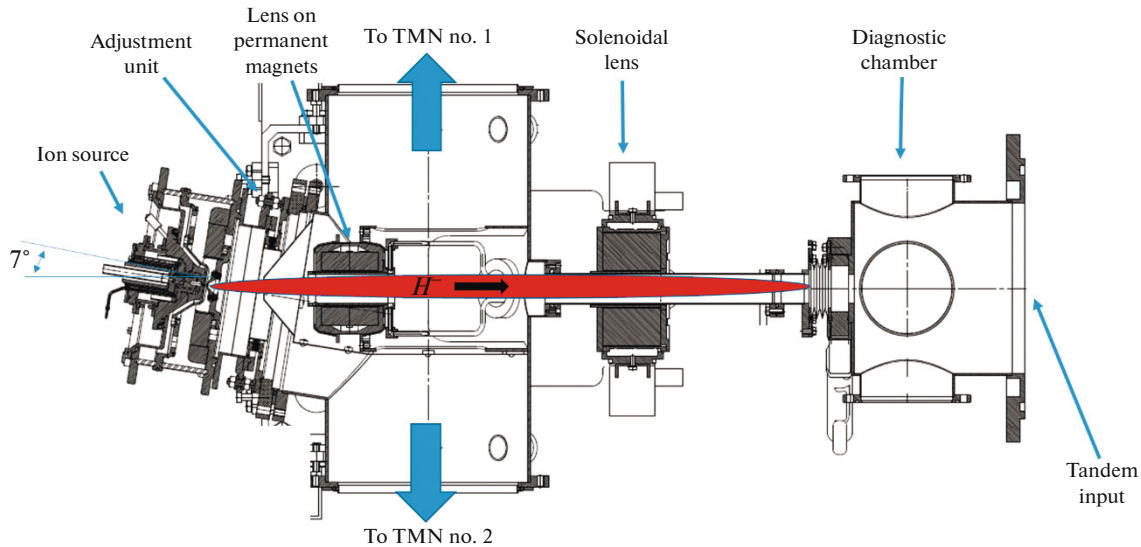
Fig. 1. BNCT tandem injector diagram. Ion source, differentially pumped chamber with permanent magnet lens, LEBT transport channel with solenoid lens. A diagnostic camera is installed at the entrance to the tandem. The red lines show the trajectories of the 32 keV ion beam as it travels from the current source to the accelerator input (COMSOL calculations).

the ion source to the accelerator input (COMSOL calculations).

3. NEGATIVE ION SOURCE

Compared to the original version of the source [1], which operated in tandem from 2006 to 2021, the new injector is equipped with a source with massive heat-resistant electrodes of the gas discharge chamber and the ion-optical system (IOS) for beam extraction and shaping. To generate a magnetic field, an internal magnetic system with permanent magnets located in a vacuum is used [3]. To increase the intensity of ion generation, the magnetic field of the source in the Penning discharge region was enhanced by installing additional permanent magnets made of NdFeB. In the new injector, the axis of the ion source is located almost horizontally (at an angle of 7° to the horizontal), while the axis of the cesium furnace (not shown in Fig. 1) is oriented almost vertically. The gas system of the source uses a two-channel hydrogen supply system: a pulsed increased supply of hydrogen is used to ignite the Penning discharge, and a stationary discharge is maintained at a reduced supply after ignition.

4. ION BEAM TRANSPORTATION TO THE TANDEM INPUT

To conduct the 30-keV beam leaving the source to the tandem input, a vacuum line was used, consisting of a chamber with differential pumping and attached to it by a low-energy tract containing an external adjustable solenoid lens and correctors (Fig. 1). The magnetic field of the source and the field of the first LEBT lens were formed using permanent magnets, and the optimal passage of the ion beam through the scattered field of the source was regulated by installing a steel correction ring at the source output, weakening the magnetic field (see Fig. 2).

Calculations of the magnetic field in the source and lens on permanent magnets, as well as the passage of the ion beam through the low-energy path of LEBT, were performed using the COMSOL code. The influence of the correction ring on the calculated trajectories of the ion beam in the section from the source to the entrance to the lens on permanent magnets is shown in Fig. 2. In the absence of a correction ring,
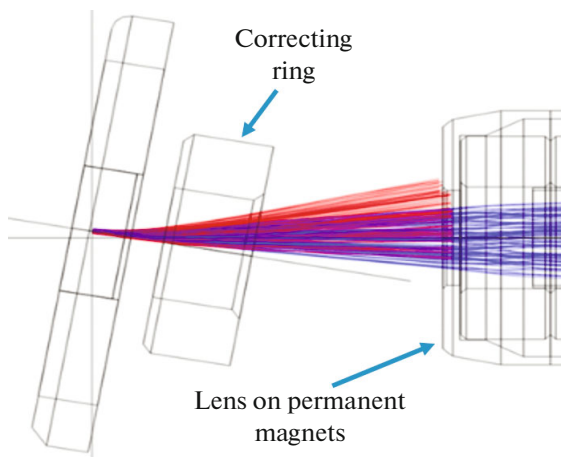

Fig. 2. Effect of magnetic field correction ring on beam rotation with an energy of 30 keV before entering the first lens. Red lines are trajectories without a corrective magnetic ring, blue lines are trajectories with a ring of optimal thickness (beam rotation angle 7°).
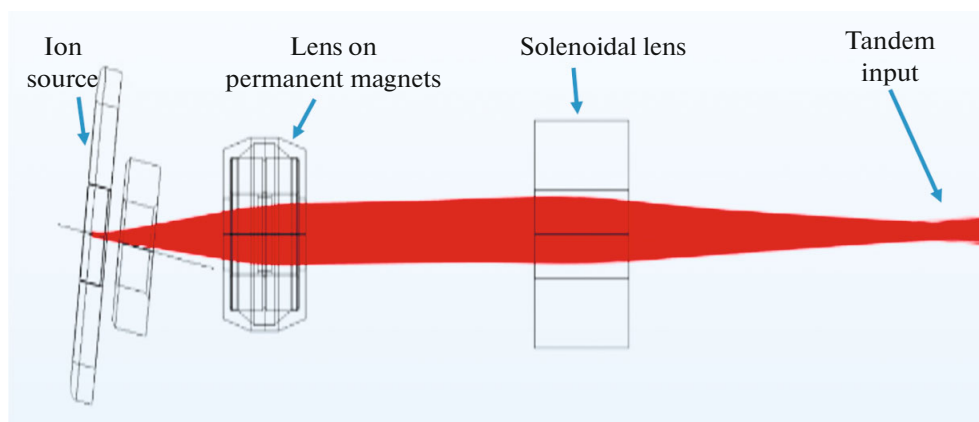
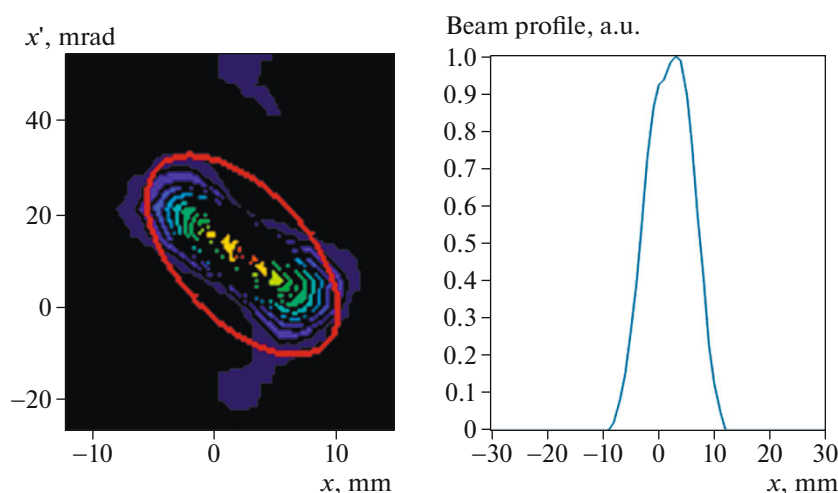**Fig. 3.** Calculated trajectories of a 32 keV ion beam during transport from the source to the tandem input.

Fig. 4. XX'-portrait on the phase plane and X-profile of a ion beam.

the ion beam is deflected at a larger angle and does not enter the aperture of the magnetic lens (red lines in Fig. 2). When installing a correction ring of optimal thickness (determined by calculations in COMSOL), the peripheral magnetic field of the source decreases faster and provides the required beam rotation angle 7°, and the ion beam itself completely flies through the magnetic lens (blue lines in Fig. 2).

To focus the beam at the entrance to low energy path LEBT, a lens consisting of two NdFeB rings magnetized parallel to the central axis was installed in the differential pumping chamber of the source. The magnetic field of the rings is directed towards each other. The magnetic flux of the rings is collected by an external yoke made of soft magnetic steel. The maximum longitudinal magnetic field on the lens axis is 0.3 T, and the minimum beam size with an energy of 32 keV is achieved at a distance of 700 mm from the lens center. A water-cooled tube with an internal diameter of 50 mm is inserted inside the rings.

The results of calculations of the transport of a beam with an energy of 32 keV through LEBT with focusing by the first lens (on permanent magnets) and the LEBT solenoidal lens are shown in Fig. 3. As can be seen in the figure, the ion beam passes well through the LEBT and is focused at the entrance to the tandem.

5. BEAM EMITTANCE

The beam emittance measurement was performed using a commercial emittance meter from D-Pace [4]. Figure 4 shows the phase XX'-portrait and X-profile of a beam of negative hydrogen ions with a current of 7 mA and an energy of 28 keV, measured at a distance of 1200 mm from the exit from the source. Due to focusing by a solenoidal lens, the beam converges and on the phase plane XX' has an average tilt angle of +10.8 mrad. In the area marked by the red ellipse, the calculated normalized RMS emittance has a value of 0.26 mm mrad. By coordinate X, the bundle is bell-
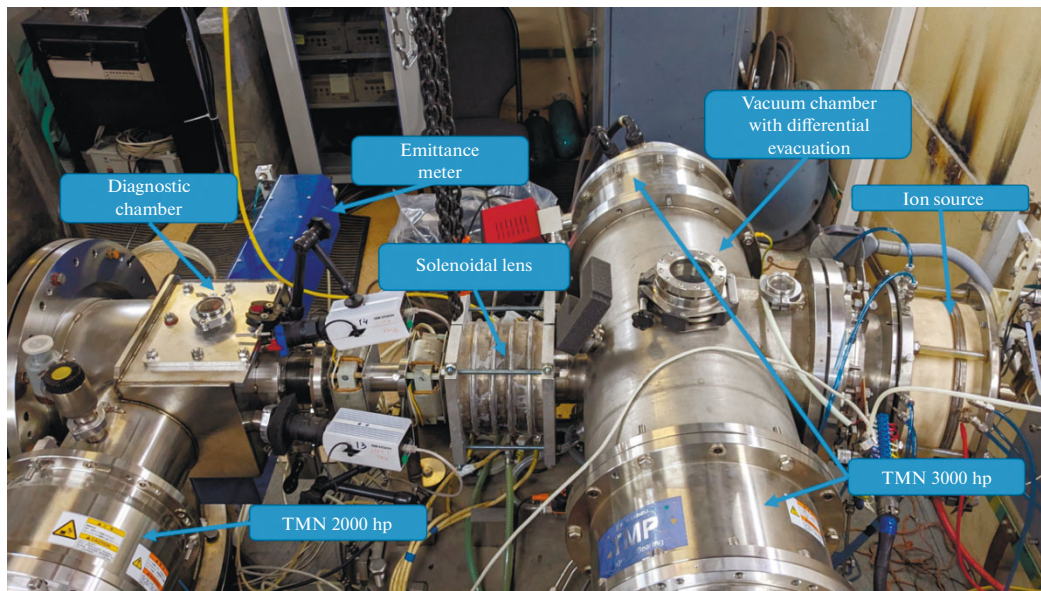
Fig. 5. Negative ion injector on BNCT tandem.

shaped and has a full width at half height (FWHA) of 11 mm.

6. STARTING AND OPERATION OF THE INJECTOR ON THE TANDEM

The negative ion injector was installed on the tandem accelerator neutron source for BNCT at the Budker Institute of Nuclear Physics, Siberian Branch, Russian Academy of Sciences (Fig. 5).

From February 2022 to July 2023, the injector worked 176 shifts, with an integral operating time of 844 h. When the injector was started, an ion beam with a current of 4.5 mA and an energy of 28 keV was conducted to the tandem input; the proton current at the tandem output was 2.3 mA, and the current on the lithium target was up to 1.9 mA. After optimizing the source by introducing additional cooling of the cathode and turning the cesium furnace of the source to a vertical position, the proton current at the output of the tandem was increased to 3.4 mA and that on the lithium target to 2.9 mA, which was sufficient to conduct experiments at the BNCT facility in 2023.

7. OBTAINING A BEAM OF NEGATIVE DEUTERIUM IONS

To conduct experiments on the generation of neutrons in the reaction of deuterium ions with lithium $D^+ + Li$, the source working gas was replaced with deuterium, and the source was reconfigured to operate with a deuterium beam. No special optimization of the ion source was carried out when working with deuterium.

To transport heavier negative deuterium ions through the source's diffuse magnetic field and the LEBT low-energy path, the energy of the negative deuterium ions was reduced to 14 keV by halving the accelerating electrode voltage. The calculated trajectories of satisfactory passage of a beam of deuterium ions with energy reduced to 14 keV through the differential pumping separation cone and the lens are shown in Fig. 6.

Table 1 presents a comparison of the ion source modes when operating with hydrogen and deuterium in the 2023 working cycles.

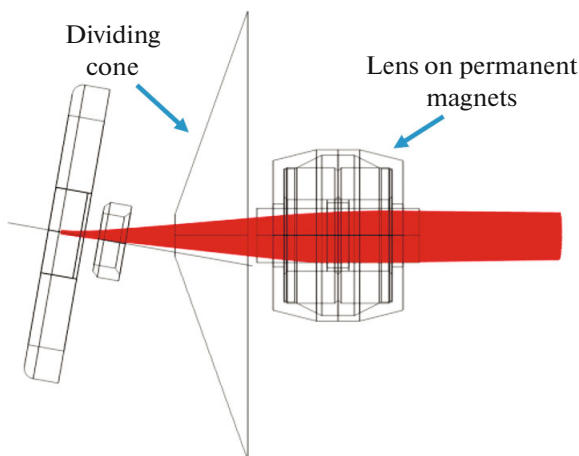As shown in Table 1, the current of accelerated protons conducted to the lithium target when working

Fig. 6. Calculated trajectories of a beam of deuterium ions with an energy of 14 keV passing through a differential pumping separator cone and through a lens with permanent magnets.

Table 1. Comparison of ion source operating modes

Gas type	Discharge			IOS Parameters				On target
	U_d, V	I_d, A	Gas flow, rel. units	U_1, kV	U_2, kV	I_1, mA	I_2, mA	I_t, mA
Deuterium	87	6	97	1.3	13	15	3	0.96
Hydrogen	90	6	104	1.3	27	9	5	1.25

with deuterium was 1.3 times lower than when working with hydrogen, which is in good agreement with the previously observed isotopic effect in the generation of a beam of hydrogen and deuterium ions in a pulsed Penning SPS [5]. The maximum current of negative deuterium ions at the input to the tandem was 3 mA, and the proton current on the lithium target reached 1.5 mA. In a cycle of daily experiments, the source operated stably on deuterium for 6−8 h a day.

8. CONCLUSIONS

An upgraded negative ion injector for the tandem accelerator has been created and launched. A focused beam of negative hydrogen and deuterium ions was obtained and accelerated in tandem; the operation of the ion source was debugged according to PC scenarios. In the mode with a low cesium feed, beams of negative hydrogen and deuterium ions with a current of 7−8 mA and 3 mA, respectively, were obtained.

FUNDING

CONFLICT OF INTEREST

The authors of this work declare that they have no conflicts of interest.

REFERENCES

1. Ivanov, A.A., Sanin, A., Belchenko, Yu., et al., *AIP Conf. Proc.,* 2021, vol. 2373, p. 070002. https://doi.org/10.1063/5.0057441

2. Sanin, A., Belchenko, Yu., Gusev, I., et al., *AIP Conf. Proc.,* 2018, vol. 2052, p. 050012. https://doi.org/10.1063/1.5083766

3. Belchenko, Y.I., Gorbovsky, A., Ivanov, A., et al., *AIP Conf. Proc.,* 2013, vol. 1515, no. 1, p. 448. https://doi.org/10.1063/1.4792815

4. Bykov, T.A., Kasatov, D.A., Kolesnikov, Ia.A., et al., *Instrum. Exp. Tech.,* 2018, vol. 61, no. 5, p. 713. https://doi.org/10.1134/S0020441218050159

5. Belchenko, Y.I. and Kupriyanov, A.S., *AIP Conf. Proc.,* 1992, vol. 287, no. 1, p. 255. https://doi.org/10.1063/1.44788